

**A Minnesota Automated Plate Scanner Catalog of Galaxies
behind the Virgo Cluster and toward its Antipode**

G. Lyle Hoffman

Dept. of Physics, Lafayette College, Easton, PA 18042; hoffmang@lafayette.edu

John M. Dickey

Dept. of Astronomy, University of Minnesota, Minneapolis, MN 55455;

john@astl.spa.umn.edu

Nanyao Y. Lu

IPAC 100-22, California Institute of Technology, Pasadena, CA 91125; lu@ipac.caltech.edu

and

René Fromhold-Treu

Dept. of Physics, Lafayette College, Easton, PA 18042; fromholdr@lafayette.edu

To Appear in the Astrophysical Journal

Received _____; accepted _____

ABSTRACT

We present a catalog of 1268 galaxies, essentially complete to $B \leq 17.0$, found by scanning glass copies of several fields of the original Palomar Sky Survey using the Minnesota Automated Plate Scanner in its isodensitometric mode (as opposed to the threshold densitometric mode used in the *APSS Catalog of the 1°0,5',5" I*). In addition to the different scanning mode, we have employed a different star-galaxy separation method and have visually inspected POSS prints to verify that each image remaining in the catalog is HII-stellar. The scanned fields are distributed generally in two areas, one around the outskirts of the Virgo Cluster, the other toward the antipode of the cluster (but still in the northern celestial hemisphere). The catalog gives the position of the center of each galaxy; estimates of the blue and red magnitudes within the outermost threshold crossing and of the blue magnitude extrapolated to zero surface brightness; blue and red diameters of four ellipses fit to the four threshold crossings (approximately 23.8, 23.6, 23.2, and 22.7 mag per square arcsec in blue, and 22.5, 22.4, 21.5 and 21.2 mag per square arcsec in red), and the ellipticities of those four ellipses. The catalog has served as a base from which to draw targets for a Tully-Fisher study of the Virgocentric infall velocity of the Local Group.

Subject headings: Catalogs Galaxies: Photometry Galaxies: Clusters: individual (Virgo)

1. Introduction

Existing galaxy catalogs, such as RC3 (de Vaucouleurs et al. 1991), UGC (Nilson 1973), and CGCG (Zwicky, Herzog & Wild 1961-1963), are quite complete at the bright end of galaxy luminosities, but much less complete at their fainter limits. For the purposes of separating out the Virgocentric component of the Local Group's peculiar velocity from the general Hubble flow and minimizing the Malmquist bias in measurements of distance within the Local Supercluster via the Tully-Fisher ("TF") method (Tully & Fisher 1977), it is important to start with a galaxy catalog that is as complete as possible, with well-specified selection criteria. To bolster the faint end completeness, and to extend the magnitude limit to somewhat fainter magnitudes, we scanned glass copies of Palomar Sky Survey (POSS) plates using the Minnesota Automated Plate Scanner (MAPS Pennington et al. 1993). The scanner provides us with a catalog of galaxies, complete to a much fainter limiting magnitude ($B \sim 17$ for the purposes of this paper, although the scanner can identify galaxies much fainter still) with accurate positions, diameters at four brightness levels, and approximate magnitudes from both blue and red plates. Throughout this paper we will use "B" to represent apparent magnitudes obtained from the POSS O plates, and "R" for those obtained from the POSS E plates.

We have scanned the sky in two general areas, one in the general direction of the Virgo Cluster and the other more or less toward the antipode. The generated galaxy catalog has been used in a recent pair of papers (Lu et al. 1993 [JIGRL] and Lu, Salpeter & Hoffman 1994 [1, S11]) to supplement a brighter galaxy sample from the Center for Astrophysics Redshift Survey ($B_T \lesssim 14$ mag; Huchra et al. 1983) to assess the shape of the dispersion about the Tully-Fisher relation in an attempt to separate out the Virgocentric component of the Local Group's peculiar velocity from the general Hubble flow using two samples of galaxies near the nominal edges of the Local Supercluster.

In future work, we intend to extend the study to galaxy groups within a somewhat larger volume on each side of the sky. Here also it will be important to make our catalog of galaxies as complete as possible for each group, and we will explore to what extent the inclusion of fainter, more irregular systems increases the accuracy of the TF distances to each group, by augmenting the number of data points in each group, and 10 what extent the accuracy is degraded by the more uncertain inclinations and wider intrinsic scatter for the more irregular systems. We hope to identify the optimal morphological type selection criteria.

The 21 cm $11\ 1$ observations and some I-band CCD photometry of galaxies from this catalog have been given in our previous papers (LII GRL and LSH). Here we describe the scanning procedure, present a B-band photometric calibration of the magnitudes obtained from the scanner, and tabulate the detected galaxies. The remainder of the paper is organized as follows: In §2, we detail the particular portions of the sky covered by this catalog, describe the scanning and data processing, give a photometric calibration of the data, and present the resulting catalog. We compare our magnitudes with those available in RC3 and discuss the completeness of the catalog in §3. Finally, we summarize our results in §4.

2. Data Acquisition and Calibration

2.1. Plate Scanning

In LSH we considered two volumes of space, dubbed BV (Behind-Virgo) and AV (Anti-Virgo), and defined as follows: BV was restricted to $1\ 0^h 30^m < \alpha < 1\ 3^h 30^m$, $0\ \text{deg} < \delta < 20\ \text{deg}$, $2500 < V_{\odot} < 4500\ \text{km s}^{-1}$; AV to $22^h < \alpha < 2^h$, $0\ \text{deg} < \delta < 20\ \text{deg}$, $V_{\odot} < 3000\ \text{km s}^{-1}$. Bright galaxies (the ‘‘CfA’’ sample of LSH) were selected from the

entire volume in each case, fainter candidates were chosen from the scanning of four complete POSS plates in the AV area and three in the BV area, along with the environs of seven groups, each having ≥ 4 members in the CfA redshift survey catalog (Huchra et al. 1983), identified by Geller & Huchra (1983) in the AV and BV volumes. For the group environs, we did not in general scan the entire POSS plate on which the group lay; rather, we scanned only a rectangular area just sufficient to include the known bright members of the group (with a small margin for safety). The particular fields scanned are detailed in Table 1.

EDITOR: PLACE TABLE HERE.

The plate scanner was used in its isodensitometric mode following procedures spelled out in Dickey et al. (1987, hereafter DKPS). In brief: the scanner recorded positions on each plate (red and blue simultaneously) where the percent transmission crosses each of four predetermined thresholds. Ellipses were fit to the threshold crossings, and the positions and ellipticities of each ellipse are recorded for (a) those whose centers coincide within $2''$ on the red and blue plates, or (b) those with good agreement between blue and red diameters in the range of 2.8 to $200''$ with a center-to-center separation greater than $2''$ but less than $30''$, with equal weight given to separation and diameter difference in choosing the best match. Positions are calibrated against SAO stars. Broken images (hereafter called "clumps," common for large diameter galaxies, especially late-type spirals and irregulars) are combined, and star-galaxy discrimination performed, as described in DKPS. However, each object in our final catalog was checked visually by one of us (GLH or RFT) to verify that it appears non-stellar on a POSS print.

2.2. B-band and CCD Photometry of MAPS Galaxies

During our main I-band CCD photometry campaign in LHGR1, we also managed to obtain, on a photometric night, B-band imaging photometry of 17 MAPS galaxies. A filter with a central wavelength of 4300Å and a FWHM of 700Å was used to mimic the Johnson B filter. The procedure of the observation, which was carried out with the Palomar¹ 200'' telescope equipped with the Four Shooter, is identical to that described in LHGR1. The resulting photometry was tied into Johnson B system via observations of standard stars in Landolt (1983).

The same surface photometric analysis as in LHGR1 was carried out on each of the CCD images by fitting elliptical contours to the galaxy image. Good fits were obtained down to a surface magnitude of 26 B mag arcsec⁻². The resulting surface brightness as a function of the semi-major axis was used to derive a mean ellipticity of the outer part of the galaxy dominated by its exponential disk; B_{26} , the isophotal magnitude at the 26th surface magnitude; and a total magnitude, B_{tot} , by extrapolating the fitted exponential disk to the infinite surface magnitude. We summarize our results in Table 2 with the following parameters: the optical morphology, taken from the RC3 or classified by us on the B band CCD image; an inclination angle, derived from the mean disk ellipticity as described in LHGR1; the major axis at the 26th surface magnitude; B_{26} ; and B_{tot} . The typical statistical error of these magnitudes is estimated to be of the order of $\lesssim 0.05$ mag.

EDITOR: PLACE TABLE 2 HERE.

¹Observations at the Palomar Observatory were made as part of a continuing collaborative agreement between the California Institute of Technology and Cornell University

2.3. Photometric Calibration of MAPS Data

Photometric calibration was performed against the CCD photometry described above for several spiral galaxies on some of the scanned plates. The number of calibrators on each plate is listed in Table 1; in particular, due to non-photometric skies above Mt. Palomar during our scheduled BV time, there are no calibrators on any of the BV plates. Ellipses were fit to isophotes on the CCD images; matching the areas of those ellipses to those fit to the MAPS threshold crossings allowed us to determine the threshold isophotes on each of the plates with calibrators. We have too few calibrators on each of CGCG fields 453, 381, 409, 410 and 385 to determine whether or not there are statistically significant differences among them, and so in the end we have simply averaged the results for those several plates. The thresholds we obtained are $23.84 \pm .06$, $23.6(1) \pm .06$, $23.204 \pm .04$, and $22.704 \pm .07$ mag [$^{\circ}$] $^{-2}$. The errors in the mean are probably fortuitously small, since plate-to-plate variations of up to 0.5 mag are expected. The eight calibrators on CGCG field 411 gave threshold isophotes that are fainter by a marginally significant amount: $24.2 \pm .3$, $23.9 \pm .2$, $23.5 \pm .1$, and $23.0 \pm .2$ mag [$^{\circ}$] $^{-2}$. Lacking information on calibration for the remaining fields, we used the less uncertain set from the set of five fields, with the intention of comparing to catalogued total magnitudes after the fact.

Given calibrated threshold levels, we have additional uncertainty in integrating over the surface density to obtain a galaxy-wide magnitude for each galaxy. A well-defined minimum luminosity (maximum magnitude) results from the assumption that the area 1)ctw' cell each pair of threshold ellipses has a constant surface brightness at the level of the outer threshold, with zero surface brightness outside the lowest threshold. We call this maximum magnitude B_{24} since the outermost threshold is approximately 24 mag [$^{\circ}$] $^{-2}$. Comparison of one of our fields (CGCG 437) with data obtained in threshold densitometric scanning mode made available on-line by the MAPS group (Pennington et al. 1993) indicates that our B_{24}

corresponds closely to the magnitudes reported by MAPS: $\langle B_{APS} - B_{24} \rangle = 0.044 \pm .045$.

We have also attempted to extrapolate from the threshold crossings to a total galaxy magnitude assuming an exponential disk in each galaxy (since we are primarily interested in spiral and irregular galaxies). This procedure is not so well-defined as that used to determine B_{24} . For regions between two thresholds, we simply used the average surface magnitude. For the region outside the faintest threshold, we extrapolated a linear fit to the four threshold crossings and integrated over the exponential distribution from the outermost threshold to infinity. For the region inside the brightest threshold (for those galaxies that crossed all four thresholds) we assumed the average surface magnitude obtained within that threshold for all the calibrators: 21.984 ± .13 for a threshold at 23.0 mag [“]-2, appropriate for CGCG field 411, and 21.74 ± .13 for the other plates (threshold 22.7 mag [“]-2). We call this estimate B_{tot} in the hope that it will approximate B_T calculated as in RC3. The resulting estimates B_{24} and B_{tot} are reported below.

We have no R-band surface photometry at all. Consequently we are not able to provide independent calibration of the red plate threshold crossings. However, we can attempt a crude calibration by comparing our results to those provided over the World Wide Web (WWW) by the MAPS group (Pennington et al. 1993). Magnitude differences between the red threshold crossings were assumed to be the same as those determined by DKPS for a different plate, and then the zero point was adjusted for each plate to minimize the difference in resulting magnitudes from those provided on WWW. This was possible for the nine plates we have in common with those available on WWW as of 21 June 1996 (CGCG fields 065, 069, 097, 407, 408, 409, 436, 437, and 460). These 9 plates give mean thresholds of 22.52, 22.42, 21.52 and 21.15 mag [“]-2 with a variance of 0.26 mag [“]-2 among the plates. For the remaining plates we simply used these mean thresholds. We constructed a red magnitude, $R_{22.5}$, from the red till the “100%” ellipses in the same manner as B_{24}

was constructed for the blue. In 20 cases among the 1268 galaxies in our final catalog, the blue galaxy image was matched to a much fainter red image, presumably an unrelated star or a small fragment of a broken galaxy image. For these 20 galaxies we report no red data at all.

2.4. The suits

In preparing our final catalog, we considered: (1) all images whose outermost threshold crossings are larger than 200 microns on the blue plates; (2) all “clumped” images; (3) all images that crossed all four thresholds, passed our star-galaxy separation tests, and have $B_{tot} < 17.0$. We did not find any images that failed to cross the highest threshold yet still were brighter than $B_{tot} = 17.0$. All images were checked on a copy of the POSS prints, and our catalog below includes only those that were judged by eye to be non-stellar. Our magnitude limit of 17.0 by no means represents the faintest that MAPS is capable of detecting, but since we are primarily interested in nearby galaxies and wished to keep stellar interlopers to a minimum, we chose not to push to a fainter limit for this survey.

The galaxies found by MAPS are presented in Table 3. Entries are ordered by CGCG field, in order of the right ascension of the field center, and then by galaxy right ascension within each field. There are two lines for each galaxy. Column (1) in the table gives a running reference number within each CGCG field. Another name by which the galaxy is known in other catalogs follows in column (2); here “U” refers to UGC; “N” to NGC and “I” to IC; “X” is short for Zwicky, i.e., CGCG; and “Mk” denotes a galaxy from the Markarian et al. (1989) lists. The right ascension of the center of the outermost ellipse, in the format hh.mmss, is given in column (3), with the corresponding declination in column (4). Our estimate of the maximum magnitude B_{24} (minimum luminosity) consistent with the threshold crossings on the blue (red) plate is given in the upper (lower) line of

column (5), with our estimate of the total magnitude B_{tot} in column (6). For the remaining columns, the first line for each galaxy gives data from the blue (O) plate, with data from the red (E) plate in the second line. For the few galaxies for which we have no red data, zeroes are recorded in line 2. The diameters of circles with areas equal to each of the four ellipses fit to the threshold crossings are given in the next four columns, (7)–(10), in units of arcseconds. In the case of clumped images, the diameter is that of a circle equal in area to the sum of all ellipses in the clump at the corresponding threshold. Columns (11)–(14) contain the ellipticities of the four ellipses; in the case of clumped images, only the outermost ellipticity is given.

EDITOR: PLACE TABLE 3 HERE.

3. Catalog Statistics

3.1. Comparison to other published magnitudes

To test the reliability of our magnitude estimates, we have performed linear regression analyses against magnitudes listed in RC3. Regressions were performed separately for B_{tot} against photoelectrically measured B_T and for B_{tot} against the combined sample of B_T (when available) and photographically determined m_B (for galaxies for which B_T is not available). Since the results for regressions against B_T alone are entirely consistent with those for the larger B_T plus m_B sample, we summarize only the latter here. In what follows, “ m_B ” is short for “ B_T or m_B ”.

For 123 galaxies in the BV region, spanning $11 < B_T < 16.5$, we find $B_{tot} = (1.34 \pm 0.65) + (0.950 \pm 0.046) m_B$, over the range of available m_B . B_{tot} is fainter on average by an amount ranging from 0.79 mag at the bright end to 0.50 mag at

the faint end. The A_V region gives similar results: for 158 galaxies spanning the same range of m_B , WC find $B_{tot} = (1.36 \pm 0.58) + (0.946 \pm 0.039)m_B$, with B_{tot} fainter than m_B 011 average by 0.77 at the bright end and 0.47 at the faint end. Evidently our extrapolation of the surface brightness beyond the outermost threshold has underestimated the outer luminosity significantly. As Figure 1 attests, no significant difference between the A_V and B_V volumes can be discerned within the scatter, so it appears that our calibration is acceptable even on plates where we have 110 calibrators; a similar comparison between individual plates indicates that our results are consistent with there being plate-to-plate variations in threshold crossings of 0.3 to 0.5 mag, but we cannot offer a statistically significant adjustment for individual plates based on these comparisons alone.

EDITOR: PLACE FIGURE 1 HERE.

That we have underestimated the outer luminosity in some, if not all, galaxies is confirmed by comparison of our B_{tot} to that estimated directly from the CCD photometry for the set of 17 calibrators (only 15 of which could be matched to MAPS images). For the set, we find $\langle B_{tot}(\text{MAPS}) - B_{tot}(\text{CCD}) \rangle = 0.32$ with a standard deviation of 0.33. The CCD B magnitudes for the calibrators are, on average, 0.14 mag (standard deviation 0.18 mag) fainter than the RC3 magnitudes for those same objects.

3.2. Catalog Completeness

While it was our intention to produce a complete, magnitude-limited catalog, comparison of our Table 3 with other catalogs of galaxies (CGCG and UGC in particular) spanning the same areas of the sky indicates that in a few fields we have missed some *bright* galaxies. The particular fields are CGCG 408-410, 041, 069 and 043, all scanned during our first session with the scanner (1989 October). We are not sure why these galaxies were

missed by the scanner, and by the time the problem was discovered it was not possible to return to the scanner to investigate the cause. We note, however, that this problem with recognizing large galaxies is not unique to MAPS (Lovejoy 1996). The missed galaxies span the full range of magnitudes in the UGC and CGCG; there is no apparent selection bias that we can discern. The data obtained from the scanner in our second session, 1990 October, do not suffer from similar missed bright galaxies. We are therefore more confident of the completeness of our catalog for the scanned portions of CGCG fields 430, 453, 381, 407, 385, 436, 437, 460, 065, and 097.

As mentioned above, we have retained all confirmed galaxy images to a B magnitude limit of 17.0, along with all large diameter and “clumped” images without regard to magnitude. How successful was our algorithm in capturing all galaxies to that magnitude limit? Have some galaxies been misclassified as stars in spite of our conservatism? To address those questions, we have produced a plot of the number of galaxies per square degree per magnitude, $N(m)$, in Figure 2. For comparison we have computed $N(m)$ using the B_{24} magnitudes which agree closely with the magnitudes tabulated by the MAPS group. The solid curve in the figure is a fit to the corresponding $N(m)$ obtained from the MAPS data for the “interfilament” (IFIL) sample of Odewahn & Aldering (1995). The IFIL sample is meant to be representative of regions outside of superclusters (or filaments in the large-scale structure) toward the North Galactic Pole. It was constructed using a neural net algorithm (Odewahn 1995) for star-galaxy separation, and is thought to be complete for galaxies to $B_{APs} \sim 20$. Although some parts of our survey cut through denser portions of the local Supercluster (and there are significant field-to-field variations), it is clear from Fig. 2 that the fainter (presumably mainly higher redshift) parts of our sample as a whole are from environments comparable to IFIL, and that we have met our intended completeness limit of $B_{tot} \sim 17.0$ (some of which will have B_{24} somewhat fainter so that the cut-off at 17.0 is not sharp in B_{24} .)

EDITOR: PLACE FIGURE 2 HERE.

4. Summary

We have employed the Minnesota Automated Plate Scanner (MAPS) to obtain accurate positions, B magnitudes and diameters, and ellipticities for a catalog of 1268 galaxies in two general areas, one around the outskirts of the Virgo Cluster and the other more or less toward the antipode. Seven 1°SS plates were scanned in their entirety (4 in the antipodal region, 3 around the Virgo Cluster), along with rectangular areas just sufficient to include all members of known galaxy groups (Geller & Huchra 1983) on 10 additional plates.

CCD photometry for a set of 17 galaxies was reported, and used to calibrate the MAPS threshold levels. An algorithm for estimating the total magnitude (extrapolated to zero surface brightness) was detailed, and the resulting magnitudes were compared to the CCD photometry of the 17 calibrators and to all magnitudes available in RC3 for these objects. Our extrapolated B_{tot} appears to be too faint by about half a magnitude on average.

The completeness of our catalog to its intended magnitude limit $B_{tot} \leq 17' . ()$, was assessed. The scanner's propensity (evidently shared with other plate scanners; Loveday 1996) for missing 10% or so of the *bright* galaxies was noted, and a plot of $N(m)$ reveals a high degree of completeness to our intended limit.

We thank E.E. Salpeter for inspiring this project, G. Aldering for providing us with electronic copy of data, R. Pennington and W. Zurek for technical support in the use of the Minnesota APS, and R. M. Humphreys for granting us time on the scanner. This work was supported in part by US National Science Foundation grants AST-9015181 and AST-9316213 at Lafayette College.

REFERENCES

- Binggeli, B., Sandage, A., & Tammann, G.A. 1985, *AJ*, 90, 1681 (BST)
- de Vaucouleurs, G., de Vaucouleurs, A., Corwin, H. (I.), Buta, R. I., Paturel, G., & Fouqué, J. 1991, *Third Reference Catalog of Bright Galaxies*, (New York: Springer-Verlag) (RC3)
- Dickey, J.M., Keller, D.T., Pennington, R., & Salpeter, E.E. 1987, *AJ*, 93, 788 (1111'S)
- Geller, M.J., & Huchra, J.J. 1983, *ApJS*, 52, 61
- Helou, G., Giovanardi, C., Salpeter, E.E., & Krumm, N. 1981, *ApJS*, 46, 267
- Helou, G., Hoffman, G.L., & Salpeter, E. E. 1984, *ApJS*, 55, 433 (1111 S84)
- Hoffman, G. L., Helou, G., & Salpeter, E.E. 1988, *ApJ*, 324, 75 (1111S88)
- Hoffman, G.L., Lewis, B. M., Helou, G., Salpeter, E.E., & Williams, H.L. 1989b, *ApJS*, 69, 65
- Hoffman, G. L., Salpeter, E.E., Farhat, B., Roos, T., Williams, H. & Helou, G. 1996, *ApJS*, in press
- Huchra, J., Davis, M., Latham, D., & Tonry, J. 1983, *ApJS*, 52, 89
- Loveday, J. 1996, *MNRAS*, 278, 1025
- Lu, N. Y., Hoffman, G.L., Groff, T., Roos, T., & Lamphier, C. 1993, *ApJS*, 88, 383 (LHGRL)
- Lu, N. Y., Salpeter, E.E., & Hoffman, G.J. 1994, *ApJ*, 426, 473 (LSH)
- Markarian, B.E., Lipovetsky, V. A., Stepanian, D. A., Prastova, L.K., & Shapovalova, A.J. 1989, *Soob. Spets. Astrofiz. Obs. No. 62*
- Nilson, P. 1973, *Uppsala General Catalog of Galaxies* (Uppsala: Acta Universitatis) (UGC)
- Odewahn, S., C. 1995, *PASP*, 107, 770

- Odewahn, S.C., & Aldering, G. 1995, *AJ*, 110, 2009
- Pennington, R.L., Humphreys, R.M., Odewahn, S.C., Zunnach, W., & Thurmes, P.M. 1993
PASP, 105, 521
- Tully, R.B., & Fisher, J.R. 1977, *A&A*, 54, 661
- Zwicky, F., Herzog, W. & Wild, P. 1961-1963, *Catalogue of Galaxies and Clusters of Galaxies*
 (Pasadena: California Institute of Technology) (CGCG)

Fig. 1.- Comparison of our B_{tot} magnitudes vs. m_B (short for " B_T or m_B ") from RC3, for the AV and BV regions separately. In each panel, the solid line shows the ordinary least-squares regression of B_{tot} against m_B , with m_B taken to be the independent variable. The dashed line has slope 1 and intercept 0 to indicate where the data points would fall if there were perfect agreement between the two magnitude estimates.

Fig. 2.- Logarithm of the number of galaxies per square degree per unit magnitude for our full sample (triangles), compared to the corresponding quantity for the IFU sample (smooth curve). Both are computed from B_{24} magnitudes.

TABLE 1
SCANNED FIELDS

Plate Center 11111"1111 + °'	R.A. Range 1111 111111- h]]	Dec. Range mm ^{0'} - °'	Area [°] ²	No. of Galaxies	Group GH	No. of Calibrators
22 53 + 1230	2249- 2301	1 3 2 0 - 1 5 3 4	6.5	35	163	· · ·
2253 + 18 30	2250- 2304	1542- 1701	4.4	21	163	1
2341 + 0030	2339-2349	0247- 0331	1.8	7	172	1
23 41 -{ 06 30	2338-2348	0340-0427	2.0	19	172	...
0005 + 06 30	2353- 0017	0327- 0928	35.9	86
0029 + 06 30	0017- 0041	0340- 0927	34.5	139	...	2
0053 + 06 30	0042-01 04	0349- 0927	30.8	36	· · ·	1
01 17 + 06 30	01 04- 01 28	0339- 0920	33.9	123	12 & 13	8
01 17 + 00 30	01 15- 01 22	0245- 0332	1.4	14	12	2
01 1741230	01 15- 0126	0937-1037	2.7	28	13	...
01 41+ 1230	01 28-0147	1213- 1522	14.5	84	17	...
0141 +- 1830	0128--0145	1546- 1923	14.7	62	17	· · ·
10 29 + 11 30	1028-1040	11 54-- 1426	7.4	55	62	...
11 41 + 17 30	11 32 - 11 46	15 16 - 1939	14.6	101	88	...
1204 + 0530	1153- 1217	0232-0829	35.5	78
1204 + 11 30	11 53 - 1217	0831-1423	34.5	238
12 52 + 05 30	1241 - 1305	0240- 0824	34.2	142	· · ·	...

TABLE 2
B-BAND CCJ) PHOTOMETRY OF MAPS GALAXIES

Galaxy	Morphology	Inclination (degree)(arcmin)	$2a_{26}$	B_{26} (mag)	B_{tot} (mag)
NGC 0488	Sb	41	5.87	11.34	11.27
NGC 7448	Sbc	63	2.70	12.27	12.23
NGC 0474	so	33	3.53	12.60	12.57
NGC 0470	Sb	58	3.19	12.78	12.67
NGC 7750	SBc	63	1.91	13.57	13.54
NGC 0489	so	80	1.71	13.74	13.73
UGC 01014	Sm	27	1.25	14.97	14.81
UGC 00634	SBdm	66	1.94	15.29	15.09
IC 0052	Sdm	68	1.01	15.22	15.19
Z411-042	Sm	60	1.22	15.40	15.29
Z409-018	Slo?	60	1.16	15.35	15.32
UGC 00964	Sb	81	1.13	15.41	15.39
UGC 00882	Sm	54	1.36	15.78	15.58
Z409-040 ^a	so	55	0.70	15.66	15.65
Z411-038	S110	40	0.77	15.94	15.80
0120+0835	SBc	16	0.84	15.93	15.84
0128+0424	Sdm	49	0.76	16.33	16.25

^athe I-band inclination angle in LUGRL appears to be more accurate.

TABLE 3
GALAXIES FOUND BY MAPS

Ref. No.	Ident.	R.A.	Dec.	B_{24} $R_{22.5}$ mag	B_{tot} mag	d_1 d_1 "	d_2 d_2 "	d_3 d_3 "	d_4 d_4 "	ϵ_1 ϵ_1	ϵ_2 ϵ_2	ϵ_3 ϵ_3	ϵ_4 ϵ_4
(1)	(2)	hh.mmss (3)	dd.minss (4)	(5)	(6)	(7)	(8)	(9)	(10)	(11)	(12)	(13)	(14)
Field 430													
1		22.49276	15.24459	16.4 14.4	16.0	25 32	23 28	18 22	11 18	0.21 0.16			
2		22.49532	15.34013	17.3 16.8	16.9	16 9	14 8	12 8	8 7	0.61 0.02			
3	U12226	22.50195	15.33012	15.7 14.6	15.2	34 28	31 26	26 21	17 17	0.52 0.46			
4		22.50311	15.16047	17.3 0.0	17.0	16 0	14 0	12 0	7 0	0.60 0.00	0.58 0.00	0.54 0.00	0.34 0.00
5	Z430-028	22.52107	15.29119	16.0 14.6	15.5	29 27	27 26	24 23	16 18	0.18 0.25			
6		22.52503	15.29303	17.4 16.2	17.1	16 14	14 12	12 10	6 8	0.20 0.27			
7		22.54061	14.37089	17.2 15.6	16.9	17 17	16 16	13 13	7 11	0.11 0.12	0.16 0.11	0.14 0.06	0.26 0.08
8		22.55237	14.28520	17.0 15.6	16.4	18 17	17 15	15 13	11 11	0.63 0.61			
9		22.55266	13.52535	17.1 15.0	16.7	18 24	16 21	13 17	8 14	0.24 0.14			
10	N7437	22.55408	14.02234	13.9 12.8	13.6	78 69	73 61	62 47	31 32	0.02 0.08			
11		22.55435	14.34532	17.1 15.5	16.6	17 17	16 16	14 14	10 12	0.68 0.63	0.67 0.63	0.64 0.65	0.54 0.60
12		22.55480	15.14000	16.9 16.0	16.6	20 16	18 14	15 10	8 8	0.32 0.39			
13	Z430-036	22.56053	14.54170	16.2 14.8	15.6	25 24	23 22	21 20	16 18	0.14 0.19			
14	Z430-037	22.56242	14.26212	16.8 15.4	16.2	20 18	19 17	16 15	12 13	0.57 0.61	0.58 0.61	0.60 0.63	0.63 0.65
15		22.56300	13.30141	17.3 15.7	16.8	16 16	15 15	13 13	9 11	0.67 0.72			
16	7/430-038	22.56329	13.32432	16.8 15.4	16.2	19 18	18 17	16 15	13 14	0.27 0.24	0.31 0.25	0.33 0.26	0.30 0.25
17		22.56378	13.27126	16.9 16.0	16.5	19 15	18 13	15 11	9 7	0.69 0.65			
18	U12281	22.56432	13.20169	14.8 13.3	14.5	52 51	48 47	40 39	21 31	0.90 0.88			
19	Z430-041	22.56576	14.53005	16.7 15.2	16.1	21 20	19 18	17 16	12 14	0.23 0.32			
20	N7442	22.56576	15.16480	14.6 13.4	14.1	53 47	51 44	45 39	32 32	0.04 0.00			
21	Z430-043	22.57062	13.49149	15.9 14.5	15.4	30 28	29 26	26 23	16 20	0.70 0.70			
22		22.57333	15.24380	16.2 15.2	16.1	29 24	25 20	17 16	7 10	0.22 0.31			
23		22.57468	13.19317	16.1 14.8	15.6	28 25	26 23	23 20	15 16	0.61 0.64	0.62 0.63	0.64 0.62	0.58 0.60
24	Z430-046	22.58164	13.21014	15.4	14.9	36	34	31	22	0.27			

TABLE 3- *Continued*

Ref. No.	Ident.	R.A.		Dec.	B_{24} $R_{22.5}$	B_{tot}	d_1 d_1	d_2 d_2	d_3 d_3	d_4 d_4	ϵ_1 ϵ_1	ϵ_2 ϵ_2	ϵ_3 ϵ_3	ϵ_4 ϵ_4
(1)	(2)	hh mmss	dd.mmss	(4)	mag	mag	(7)	(8)	(9)	(10)	(11)	(12)	(13)	(14)
		(3)	(4)		(5)	(6)								
					14.1		34	32	29	24	0.32			
25		22.58433	14.28326		16.7	16.3	21	20	17	9	0.70			
					15.1		21	20	17	15	0.71			
26	U12308	22.58490	14.04179		14.8	14.4	51	46	37	24	0.78			
					13.9		39	36	29	22	0.79			
27	X430-050	22.58591	14.19560		16.4	15.9	24	22	19	13	0.29			
					14.9		23	21	19	16	0.21			
28	N7461	22.59193	15.18478		15.9	15.4	31	28	23	17	0.47			
					14.1		36	32	27	23	0.45			
29		22.59422	14.12156		16.9	16.3	19	18	16	11	0.40			
					15.0		21	20	18	16	0.43			

NOTE. - Table 3 in its entirety may be found in machine-readable form on the AAS CD-ROM, Vol. NNN. The data for one CGCG field is shown here as a guide to the format of the table.

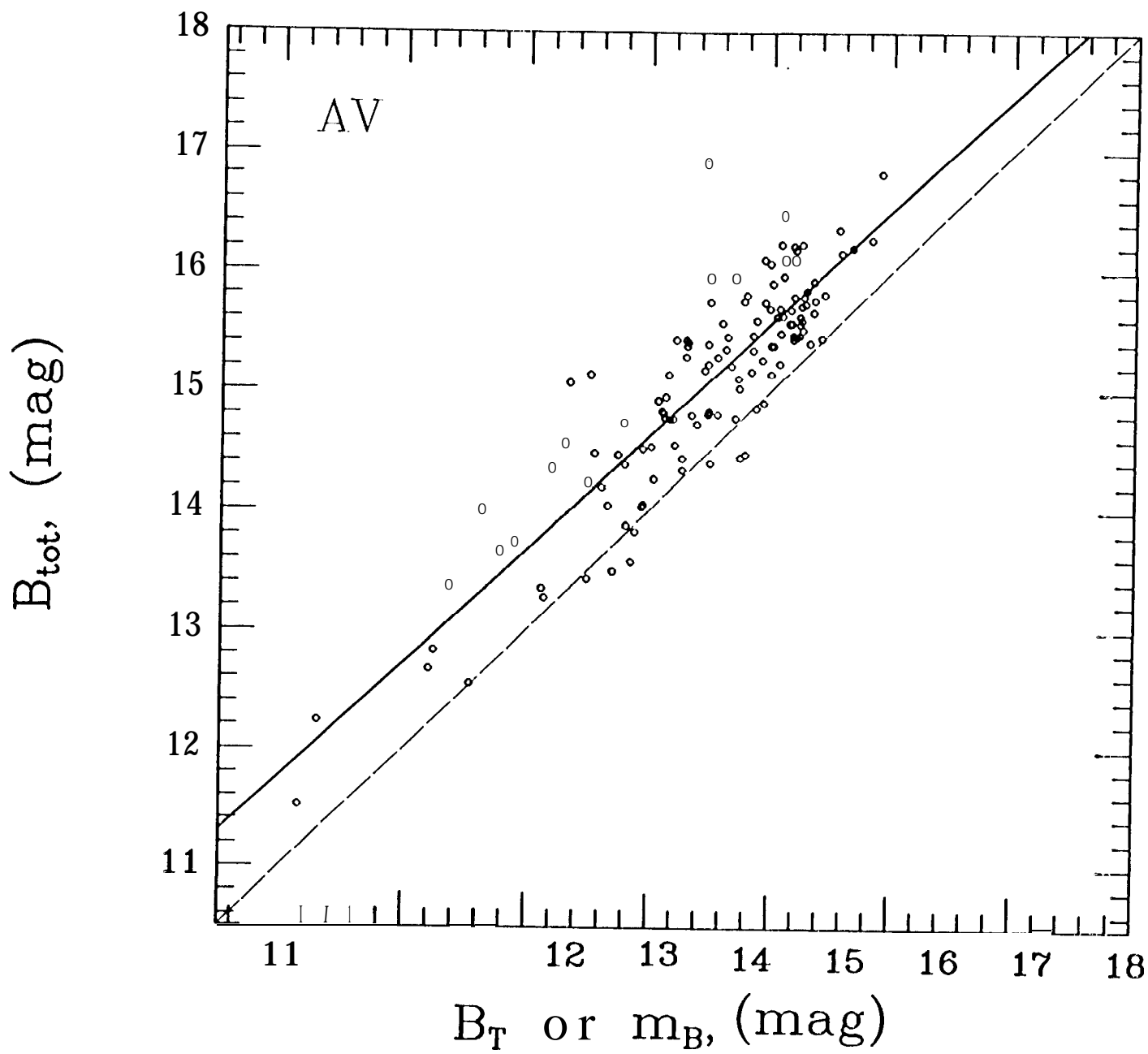


Fig. 1a

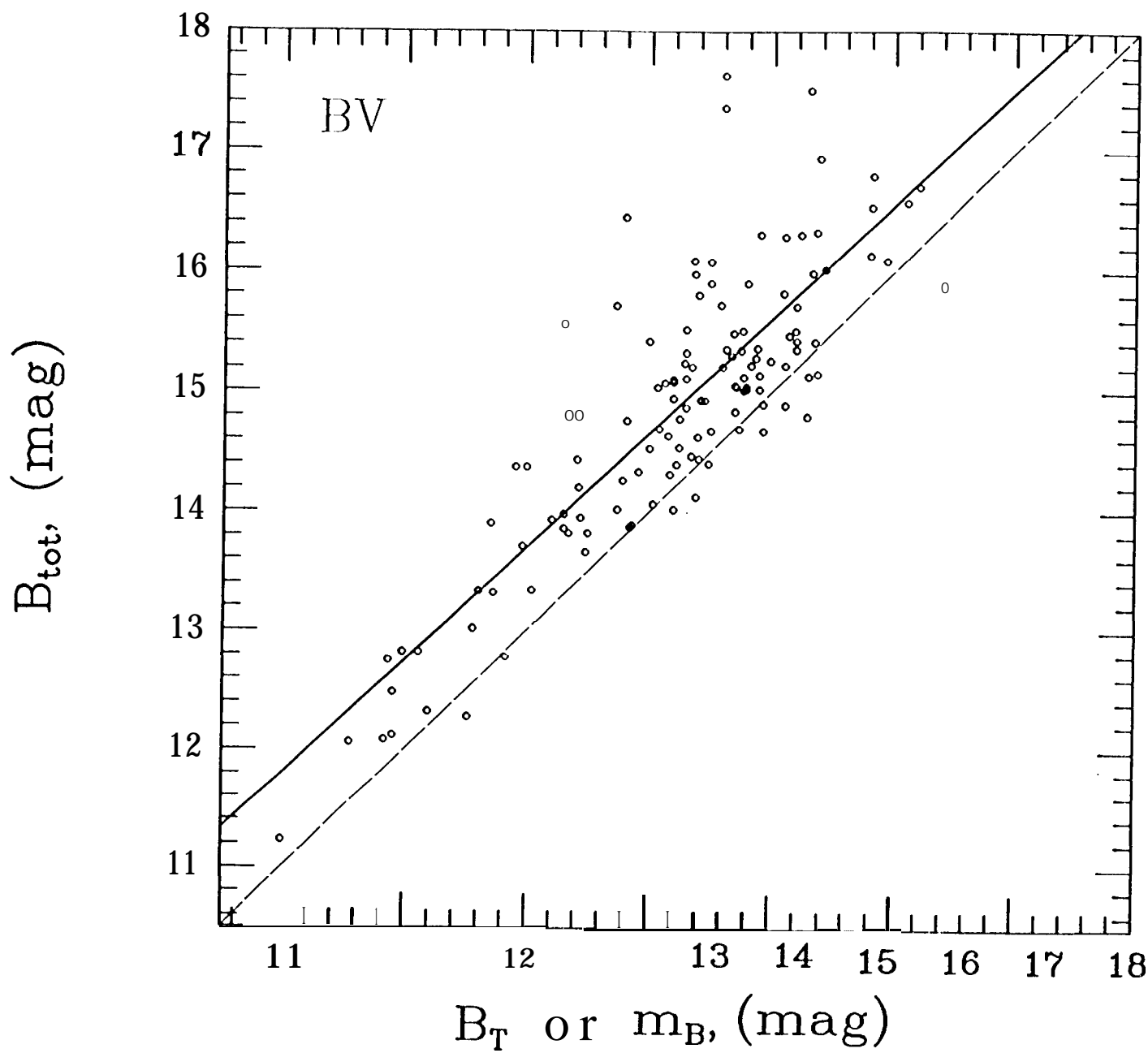


Fig. 16

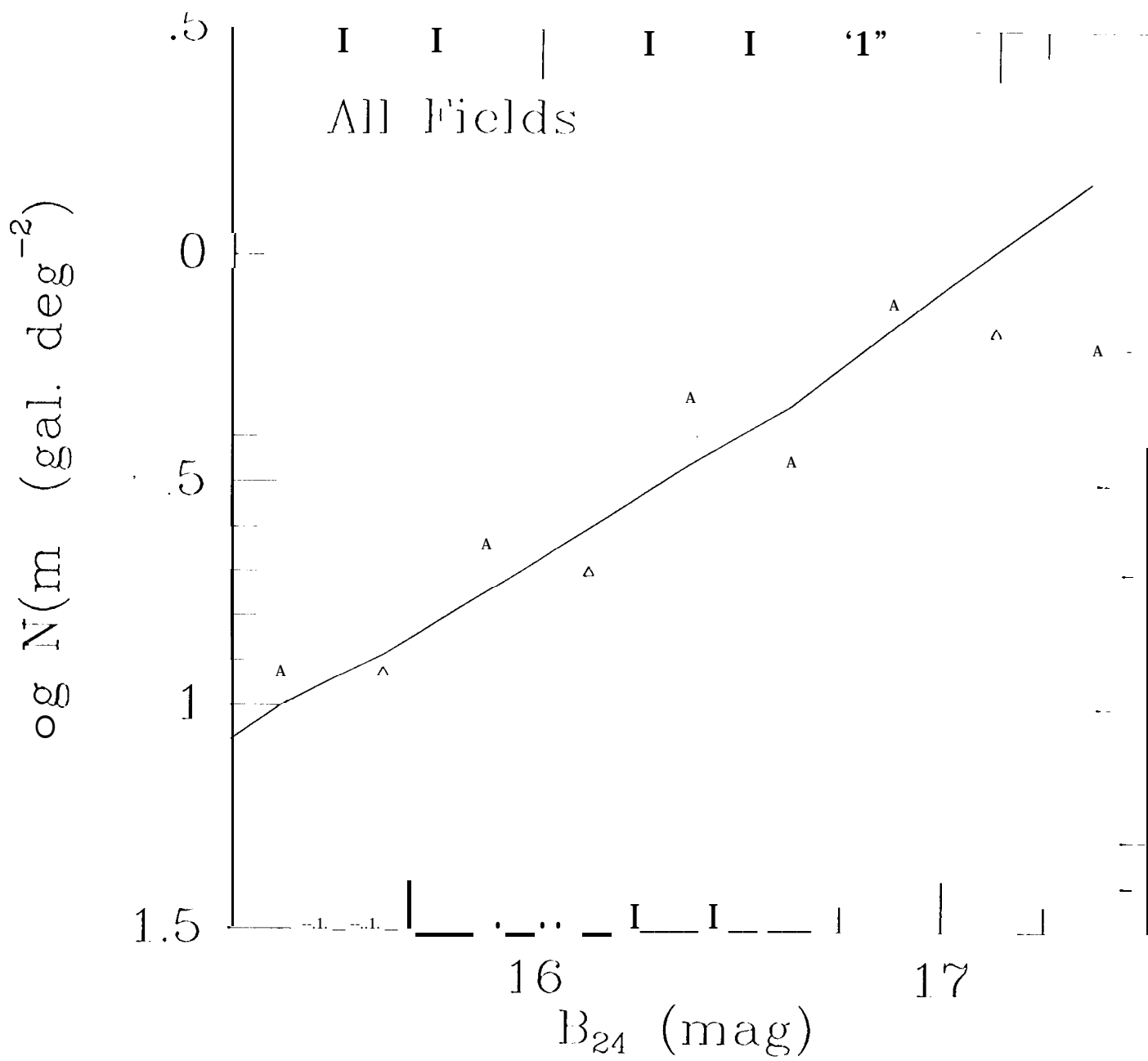


Fig. 2

A Minnesota Automated Plate Scanner Catalog of Galaxies behind the Virgo Cluster and toward its Antipode

G. Lyle Hoffman, John M. Dickey, Nanyao Y. Lu & Rent Fromhold-Treu

<1996, submitted to ApJS>

Abstract :

We present a catalog of 1268 galaxies, essentially complete to $B \leq 17.0$, found by scanning glass copies of several fields of the original Palomar Sky Survey using the Minnesota Automated Plate Scanner in its isodensitometric mode (as opposed to the threshold densitometric mode used in the APS Catalog of the POSS 1). In addition to the different scanning mode, we have employed a different star-galaxy separation method and have visually inspected POSS prints to verify that each image remaining in the catalog is non-stellar. The scanned fields are distributed generally in two areas, one around the outskirts of the Virgo Cluster, the other toward the antipode of the cluster (but still in the northern celestial hemisphere). The catalog gives the position of the center of each galaxy; estimates of the blue and red magnitudes within the outermost threshold crossing and of the blue magnitude extrapolated to zero surface brightness; blue and red diameters of four ellipses fit to the four threshold crossings (approximately 23.8, 23.6, 23.2, and 22.7 mag per square arcsec in blue, and 22.5, 22.4, 21.5 and 21.2 mag per square arcsec in red), and the ellipticities of those four ellipses. The catalog has served as a base from which to draw targets for a Tully-Fisher study of the Virgocentric infall velocity of the Local Group.

Keywords: Galaxies: Spiral --- Galaxies: Irregular --- Galaxies: Photometry
-- Galaxies: Clustering

Description :

Table 3 lists the galaxies found by the scanner in each of the 17 fields. The table is organized by CGCG field, with a local running reference number ordered by increasing right ascension within that field. B24 is our estimate of the faintest B magnitude consistent with the four threshold crossings for each galaxy, and Btot is our attempt to estimate the total B magnitude extrapolated to zero surface brightness. The diameters of circles with areas equal to the ellipses fit to the four threshold crossings are given, along with the ellipticities of those ellipses. For broken images ("clumps"), only the ellipticity of the outermost ellipse is given. On the second line for each galaxy, we give corresponding measurements of R24, diameters and ellipticities from the R plate.

File Summary:

File Name	Lrefl	Records	Explanations
table3.dat	77		Galaxies found by MAPS
table3.tex			AAS _T EX version of Table 3

Byte-by-byte Description of file: table3.dat
First line for each galaxy:

Bytes	Format	Units	Label	Explanations
1-3	I3	---	Ref. No.	Running index for each field
5-13	A9		Ident.	Name from another catalog

14- 1-1	F4 .0	h	RAh	Right ascension ([950) (hours)
18-19	12	min	RAm	Right ascension (1950) (minutes)
20-22	13	0.1 s	RA s	Right ascension (1950) (seconds)
23-26	F4 .0	deg	DEd	Declination ([950) (degrees)
27-28	12	arcmin	DEm	Declination (1950) (arcminutes)
29-31	13	0.1 arcsec	DE s	Declination (1950) (arcseconds)
32-36	F5 .1	mag	B24	B magnitude to lowest threshold
37-41	F5.1	mag	Btot	B magnitude extrapolated
42-45	14	arcsec	d1	B diameter to lowest threshold
46-49	14	arcsec	d2	B diameter to second threshold
50-53	14	arcsec	d3	B diameter to third threshold
54-57	14	arcsec	d4	B diameter to highest threshold
58-62	F5 .2	.	e1	Ellipticity, lowest B threshold
63-67	F5.2	-	e2	Ellipticity, second B threshold
68-72	F5.2		e3	Ellipticity, third B threshold
73-77	F5.2		e4	Ellipticity, highest B threshold

Second line for each galaxy:

Bytes	Format	Units	Label	Explanations
1-31	---	--	---	Blank
32-36	F5.1	mag	R24	R magnitude to lowest threshold
37-41	---	.	---	Blank
42-45	14	arcsec	d1	R diameter to lowest threshold
46-49	14	arcsec	d2	R diameter to second threshold
50-53	14	arcsec	d3	R diameter to third threshold
54-57	14	arcsec	d4	R diameter to highest threshold
58-62	F5 .2	.	e1	Ellipticity, lowest R threshold
63-67	F5.2		e2	Ellipticity, second R threshold
68-72	F5 .2	---	e3	Ellipticity, third R threshold
73-77	F5.2	-	e4	Ellipticity, highest R threshold

Notes for file: table3.dat

The set of entries for each CGCG field is preceded by a line which has "Field" in bytes 1-5 followed by the number of the field as given in CGCG (format 13) in bytes 7-9.

Throughout, B refers to quantities measured on the POSS O plate, R to quantities measured on the POSS E plate.

(End)

Lyle Hoffman [Lafayette College] 15-Mar-96

Table 3 --- The Full CDROM Version

Field 430

1	22.49276	15.24459	16.4	16.0	25	23	18	11	0.21			
			14.4		32	28	22	18	0.16			
2	22.49532	15.34013	17.3	16.9	16	14	12	8	0.61			
			16.8		9	8	8	7	0.02			
3	22.50195	15.33012	15.7	15.2	34	31	26	17	0.52			
			14.6		28	26	21	17	0.46			
4	22.50311	15.16047	17.3	17.0	16	14	12	7	0.60	0.58	0.54	0.34
			0.0		0	0	0	0	0.00	0.00	0.00	0.00
5 Z430-028	22.52107	15.29119	16.0	15.5	29	27	24	16	0.18			
			14.6		27	26	23	18	0.25			
6	22.52503	15.29303	17.4	17.1	16	14	12	6	0.20			
			16.2		14	12	10	8	0.27			
7	22.54061	14.37089	17.2	16.9	17	16	13	7	0.11	0.16	0.14	0.26
			15.6		17	16	13	11	0.12	0.11	0.06	0.08
8	22.55237	14.28520	17.0	16.4	18	17	15	11	0.63			
			15.6		17	15	13	11	0.61			
9	22.55266	13.52535	17.1	16.7	18	16	13	8	0.24			
			15.0		24	21	17	14	0.14			
10 N7437	22.55408	14.02234	13.9	13.6	78	73	62	31	0.02			
			12.8		69	61	47	32	0.08			
11	22.55435	14.34532	17.1	16.6	17	16	14	10	0.68	0.67	0.64	0.54
			15.5		17	16	14	12	0.63	0.63	0.65	0.60
12	22.55480	15.14000	16.9	16.6	20	18	15	8	0.32			
			16.0		16	14	10	8	0.39			
1.3 Z430-036	22.56053	14.54170	16.2	15.6	25	23	21	16	0.14			
			14.8		24	22	20	18	0.19			
14 2430-03"/	22.56242	14.26212	16.8	16.2	20	19	16	12	0.57	0.58	0.60	0.63
			15.4		18	17	15	13	0.61	0.61	0.63	0.65
15	22.56300	13.30141	17.3	16.8	16	15	13	9	0.67			
			15.7		16	15	13	11	0.72			
16 Z430-038	22.56329	13.32432	16.8	16.2	19	18	16	13	0.27	0.31	0.33	0.30
			15.4		18	17	15	14	0.24	0.25	0.26	0.25
17	22.56378	13.27126	16.9	16.5	19	18	15	9	0.69			
			16.0		15	13	11	7	0.65			
18 U12281	22.56432	13.20169	14.8	14.5	52	48	40	21	0.90			
			13.3		51	47	39	31	0.88			
19 2430-041	22.56576	14.53005	16.7	16.1	21	19	17	12	0.23			
			15.2		20	18	16	14	0.32			
20 N7442	22.56576	15.16480	14.6	14.1	53	51	45	32	0.04			
			13.4		47	44	39	32	0.00			
21 2430-043	22.57062	13.49149	15.9	15.4	30	29	26	16	0.70			
			14.5		28	26	23	20	0.70			
22	22.57333	15.24380	16.2	16.1	29	25	17	7	0.22			
			15.2		24	20	16	10	0.31			
23	22.57468	13.19377	16.1	15.6	28	26	23	15	0.61	0.62	0.64	0.58
			14.8		25	23	20	16	0.64	0.63	0.62	0.60
24 2430-046	22.58164	13.21074	15.4	14.9	36	34	31	22	0.27			
			14.1		34	32	29	24	0.32			
25	22.58433	14.28326	16.7	16.3	21	20	17	9	0.70			
			15.1		21	20	17	15	0.71			
26 U12308	22.58490	14.04179	14.8	14.4	51	46	37	24	0.78			
			13.9		39	36	29	22	0.79			
27 2430-050	22.58591	14.19560	16.4	15.9	24	22	19	13	0.29			
			14.9		23	21	19	16	0.21			
28 N7461	22.59193	15.18478	15.9	15.4	31	28	23	17	0.47			
			14.1		36	32	27	23	0.45			
29	22.59422	14.12756	16.9	16.3	19	18	16	11	0.40			

30 N7467	22.59583	15.17051	15.0	21	20	18	16	0.43				
			16.4	16.0	25	23	18	12	0.18			
			14.5		28	26	22	19	0.15			
31	23.00054	14.56060	17.3	17.3	17	15	11	3	0.57			
			16.0		15	14	11	8	0.58			
32	23.00246	13.40501	17.3	17.1	18	16	11	4	0.34			
			16.2		15	13	9	6	0.44			
33	23.00383	13.37161	16.9	16.4	19	18	16	10	0.45			
			15.3		19	17	16	13	0.44			
34	23.00589	14.25230	16.6	16.4	23	21	17	7	0.29			
			15.4		21	18	14	10	0.23			
35	23.00033	13.39251	17.1	16.5	17	16	14	11	0.59	0.60	0.61	0.59
			15.4	18	17		15	14	0.60	0.61	0.61	0.60

..... (see t-he actual CDROM for more contents)